Multiple-scattering theory of the surface resistivity of stepped Al surfaces

P. J. Rous*
Nanoscale Physics Research Laboratory, School of Physics and Astronomy, University of Birmingham, Edgbaston, Birmingham, B15 2TT, United Kingdom

(Received 2 August 1999; revised manuscript received 7 December 1999)

When an electrical current flows parallel to a stepped metal surface, the steps contribute to the surface-induced resistivity due to the diffuse scattering of the carriers that occurs at the step edges. In this paper, multiple-scattering theory is used to compute the surface resistivity induced by steps on the vicinal (100) surfaces of Al. The carrier scattering by the surface barrier is described by a model corrugated potential fit to the results of a first-principles calculation of the surface-induced resistivity of the unstepped surface. The Bloch states of the semi-infinite bulk are described by a layer–Korringa-Kohn-Rostoker calculation. The surface resistivity is found to be a function of the step density, η_s, and becomes a linear function of η_s for low step-edge densities. Deviation for linearity at higher step densities results from the multiple scattering of carriers between step edges.

I. INTRODUCTION

In this paper we study the surface resistivity that is induced by steps at the surface of a metal through which a current is flowing. It is well known that the adsorption of adatoms or molecules onto a metallic thin film changes the surface resistivity, ρ_s, because the adsorbates act as additional scattering centers for carriers impinging on the surface.[1,2] This is a fundamental problem in the theory of electron scattering at surfaces[3] and, as Persson has demonstrated, is closely related to the theory of vibrational damping at surfaces,[4] electronic friction,[5,6] and surface electromigration.[5,7] From a technological viewpoint, advances in miniaturization will make it increasingly important to understand the surface contribution to resistance of nanoscale metallic interconnects and devices.[8] The sensitivity of the resistivity of thin films to surface contamination also forms the physical basis for many solid-state sensors.[2]

In addition to adatoms, the presence of surface steps would be expected to alter ρ_s since the diffuse scattering of carriers at the step edges alters the momentum distribution of carriers scattered by the surface[6] and therefore makes an additional contribution to the surface resistivity. Steps have been invoked as the microscopic origin of resistivity changes that can be described in terms of the surface profile autocorrelation function.[9] However, to our knowledge there has been only one prior microscopic study of surface resistivity induced by steps, a pseudopotential/jellium calculation of ρ_s for a stepped surface modeled by removing rows of atoms from Al(100) to create a (4×1) missing-row superstructure.[10] The removal of atom rows from Al(100) was found to significantly increase the surface resistivity. This phenomenon was interpreted in terms of the additional diffuse scattering of the carriers produced by the missing row. In this paper we adopt an alternative, albeit approximate, theoretical approach that allows us to isolate the surface-induced resistivity of a single step and compute ρ_s for stepped surfaces with terrace widths that are significantly longer than could be treated by first-principles methods. In addition, by computing the surface resistivity for a range of terrace widths we are able to study how the scattering interaction between step edges influences the magnitude of ρ_s. Our approach is to use a multiple-scattering model to treat the carrier scattering by the vicinal (100) surfaces of Al, replacing the true surface potential with a model corrugated surface barrier fit to first-principles calculations. The multiple scattering of the carriers between the surface barrier and the semi-infinite bulk is evaluated to determine the effective surface reflectivity for carriers impinging on the surface from the interior of the metal.

The contribution of a step to ρ_s is related to the effective wind valence that describes the force acting on a step edge when a current flows parallel to a stepped metal surface. This is because both quantities are a measure of the effectiveness with which a step diffusely scatters the carriers incident from the bulk. Explicitly, if we consider a jellium thin film, thickness l_f, with an array of identical steps having parallel edges oriented perpendicular to the applied electric field, then the effective wind valence per unit length of the step edge, z_w, is related to ρ_s as follows:

$$z_w=\frac{\eta_e l_f \rho_s}{\eta_s \rho_b}. \tag{1}$$

Here, ρ_b is the bulk resistivity and η_e is the carrier density. η_s is the one-dimensional step density. The calculation of the wind valence for steps was the subject of a prior publication.[11]

This paper is organized as follows. In the next section we outline our theoretical approach to the calculation of ρ_s for stepped surfaces. In Sec. III the results of this method are compared to prior first-principle results for Al(100) and Al(111). The method is then used to compute the surface resistivity of stepped surfaces vicinal to Al(100).

II. THEORY

Consider a surface parallel to the *xy* plane that consists of a periodic array of steps. The step edges are all oriented parallel to the *y* axis, the *z* axis is the surface normal, and a

current flows along the surface parallel to the x axis. The stepped surface is periodic with period a along the x axis and period b parallel to the y axis and generates a set of two-dimensional reciprocal lattice vectors $\mathbf{G}=(G_x,G_y)$.

The resistivity of such a surface may be calculated by computing the momentum transfer between the surface and the carriers for carriers incident from the interior of the metal at Fermi energy, ϵ_F, with parallel wave vector $\mathbf{k}_\parallel=(k_x,k_y)$. Since the stepped surface possesses two-dimensional periodicity, the carriers are diffracted back into the bulk as a set of beams with parallel wave vectors $\mathbf{k}_\parallel+\mathbf{G}$. If the probability of reflection into beam $\mathbf{G}$ is $p_G(\epsilon_F,\mathbf{k})$ then the rate of momentum transferred to the surface for unit incident flux is $\mathbf{G}p_G(\mathbf{k})$. The total momentum transfer is obtained by integrating this quantity over all $\mathbf{k}_\parallel$, weighted by the appropriate carrier population (shifted Fermi sphere). This leads to an expression (in atomic units) for the surface-induced resistivity tensor expressed in terms of p_G,[10,12]

$$l_f\rho_s^{\alpha\beta}=\frac{1}{(2\pi)^3\eta_e^2\Omega}\int\int_{SBZ}\left[\sum_{\mathbf{G}}G_\alpha G_\beta p_G(\epsilon_F,\mathbf{k}_\parallel)\right]d^2\mathbf{k}_\parallel, \tag{2}$$

where $\alpha,\beta=x,y$, Ω is the area of the surface, and the integral is performed over the surface Brillouin zone. Equation (2) is valid where a plane-wave expansion of the carrier states can be made [see Eq. (4) below].

In order to determine the the surface resistivity from Eq. (2) the reflectivity of the stepped surface for carriers incident from the interior of the metal must be computed. Our approach for computing this quantity is adapted from that detailed in earlier publications[13,11] and will be described only briefly here.

We seek solutions of the Schrödinger equation which produce a set of incoming and outgoing Bloch states asymptotically deep in the metal:

$$\psi(\mathbf{k}_\parallel,\mathbf{r})=\phi_{\mathbf{G}}(\mathbf{k}_\parallel,\mathbf{r})+\sum_{\mathbf{G}}r(\mathbf{G},\mathbf{k}_\parallel)\phi_{\mathbf{G}}(\mathbf{k}_\parallel,\mathbf{r}). \tag{3}$$

The surface reflectivity, $r(\mathbf{G},\mathbf{k}_\parallel)$, was obtained by separately computing the reflectivity of the semi-infinite bulk, $r_b(\mathbf{G},\mathbf{k}_\parallel)$, and the surface barrier, $r_s(\mathbf{G},\mathbf{k}_\parallel)$, with respect to a matching plane $(z=0)$ just outside of the topmost plane of atoms. At $z=0$ we have

$$\psi(\mathbf{k}_\parallel,\mathbf{r})=e^{i\mathbf{k}_\parallel\cdot\mathbf{r}_\parallel}e^{iK_{Gz}^{+}z}+\sum_{\mathbf{G}}\left[\mathbf{r}_s(1-\mathbf{r}_b\mathbf{r}_s)^{-1}\right]\times e^{i(\mathbf{k}_\parallel+\mathbf{G})\cdot\mathbf{r}_\parallel}e^{iK_{Gz}^{-}z}, \tag{4}$$

where the $\mathbf{k}_\parallel$ and $\mathbf{G}$ dependence of $\mathbf{r}_s$ and $\mathbf{r}_b$ are implicit and $K_{Gz}^{\pm}=\pm\sqrt{2\epsilon_F-|\mathbf{k}_\parallel+\mathbf{G}|^2}$. The probability of nonspecular diffraction is obtained by matching the solutions of Eq. (4) to Eq. (3) to determine the amplitudes of the nonevanescent reflected Bloch states, $r(\mathbf{G},\mathbf{k}_\parallel)$.

The semi-infinite bulk reflectivities were computed using a standard layer Korringa-Kohn-Rostoker method previously applied to the problem of adatom electromigration.[13] For the periodic surface barrier, Fourier transformation of the Schrödinger equation generates a set of coupled differential equations for the scattered wave functions in terms of the Fourier components of the potential $V_G(z)$,[11]

$$-\frac{1}{2}\frac{d^2}{dz^2}\phi_{\mathbf{G}}(z)+\sum_{\mathbf{G}'}V_{\mathbf{G}-\mathbf{G}'}(z)\phi_{\mathbf{G}'}(z)=(K_{Gz}^{-})^2\phi_{\mathbf{G}}(z). \tag{5}$$

For relatively small unit cells, Eq. (5) can be solved using the close-coupling method;[14] essentially Eq. (5) is numerically integrated from outside the metal to the matching plane. This method is not suitable for the stepped surfaces considered in this paper since, for each $\mathbf{k}_\parallel$, the number of reciprocal lattice vectors $\mathbf{G}$ needed to obtain convergent amplitudes increases rapidly with the step terrace width (i.e., the area of the surface unit cell). Instead, we employ an approximate model in which the surface potential is represented by a corrugation function $\zeta(\mathbf{r}_\parallel)$ that sets the location of an infinitely repulsive barrier with periodic corrugations representing the underlying surface crystallography.[15] This model potential does not reproduce, exactly, the actual (soft) surface barrier potential. Nevertheless, we can select a corrugation function that closely mimics the actual surface reflectivity. Since this is the quantity needed to compute ρ_s, we fit $\zeta(\mathbf{r}_\parallel)$ parametrically to a first-principles calculation for the unstepped surface.

This model potential permits an approximate calculation of the surface reflectivity using the Rayleigh ansatz $[\psi(\mathbf{k}_\parallel,\mathbf{r}=[\mathbf{r}_\parallel,\zeta(\mathbf{r}_\parallel)])=0]$ and solving

$$1+\sum_{\mathbf{G}}r_s(\mathbf{G},\mathbf{k}_\parallel)e^{i\mathbf{G}\cdot\mathbf{r}_\parallel}e^{i(K_{Gz}^{-}+K_{Oz}^{+})\zeta(\mathbf{r}_\parallel)}=0 \tag{6}$$

by the GR method.[16] The surface is represented by a grid of sampling points in real space, $\mathbf{r}_\parallel$, and a finite set of reciprocal lattice vectors, $\mathbf{G}$. Then, Eq. (6) may be written as a matrix equation for r_s and, for each $\mathbf{k}_\parallel$ and $\mathbf{G}$, the surface reflectivities may be obtained by matrix inversion. Formally, this method generates an asymptotic series for the reflectivities in the number of $\mathbf{G}$ vectors. Although a detailed description of the limitations of this approach can be found elsewhere,[17] we note that it has been demonstrated that for a two-dimensional sinusoidal corrugation with a peak-to-peak amplitude h and wavelength a, the method is absolutely convergent for values of h smaller than approximately $0.19a$.[17] In fact, for the specific case of the stepped surfaces vicinal to Al(100) considered in this paper, the approximation becomes more accurate for larger terrace widths and the corrugation height is larger than this limiting value only if the (100) terraces are shorter than two atoms across. For all of the calculations presented in this paper the GR method produced surface reflectivities that obeyed the flux conservation test to within 0.1%. Consequently, the Rayleigh ansatz is not a significant source of error in our calculation.

III. RESULTS

Using the approach described in the previous section we have computed the surface resistivity of step arrays corresponding to the vicinal (100) surfaces of Al. The unstepped surface, Al(100), has a square unit cell of side $a_0=2.86$ Å and an interplanar spacing $h_0=2.02$ Å. The vicinal Al surfaces considered in this paper consist of an array of identical

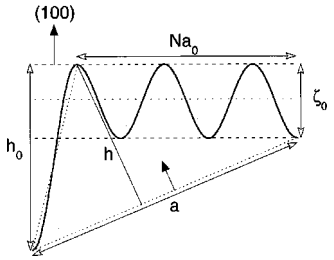

FIG. 1. The corrugation function used to describe the vicinal (100) surfaces of Al considered in this paper. $h_0 = 2.02$ Å. The (100) terraces have a sinusoidal corrugation with peak-to-peak amplitude ζ_0. The step height, h, is equal to the interplanar spacing of Al(100) projected onto the surface normal of the stepped surface.

steps with (100) terraces. These surfaces are classified as $N(100)\times(111)$ where N is the number of atoms on the terrace (including the in-step atom).[18] Note that the limit $N \rightarrow \infty$ corresponds to Al(100) while $N=1$ corresponds to Al(111). The generic corrugation function for these stepped surfaces is shown in Fig. 1. The (100) terraces are modeled by a sinusoidal corrugation with a peak-to-peak amplitude ζ_0. The step height is labeled h.

The surface reflectivity for this model surface was determined using the GR method described in the previous section. The number of $\mathbf{k}_\parallel$, $\mathbf{G}$, and $\mathbf{r}_\parallel$ vectors needed to generate converged amplitudes increases linearly with the area of the surface unit cell. In order to obtain the results described in this section we employed up to 328 symmetry inequivalent $\mathbf{k}_\parallel$ points within the surface Brillouin zone, up to 900 reciprocal lattice vectors and up to 1312 real-space sampling points.

The amplitude of the terrace corrugation ζ_0 was adjusted until the calculated surface-induced resistivity of the unstepped (100) surface of Al was equal to the value obtained from the first-principles calculation of Ishida[12] ($[l_f \rho_s^{xx}] = 0.59$ a.u.). The best-fit value of the corrugation amplitude for Al(100) was $\zeta_0 = 0.42$ Å. As a test, we then computed $[[l_f \rho_s^{xx}]$ for $N=1$; Al(111)]. We obtain a value of $[l_f \rho_s^{xx}] = 3.60$ a.u. which is in excellent agreement with Ishida's first-principles calculation of ρ_s for Al(111); ($[l_f \rho_s^{xx}] = 3.54$ a.u.). This good agreement might seem fortuitous, especially given the approximations inherent on our approach. However, the physical origin of the relatively large resistivity of Al(111) is the symmetry of the surface which, in contrast to Al(100), does not generate a specularly reflected Bloch wave.[12] Although the surface potential is treated approximately in our approach, the surface symmetry is correctly described. Therefore we expect to obtain reasonable values for the relative resistivity of Al(100) and Al(111), and we have some confidence that our approach can reproduce the trends in ρ_s for the intermediate set of stepped surfaces that are the focus of this paper.

In order to make contact with a prior study by Ishida,[10] we considered first the surface-induced resistivity of an Al(100) surface in which one in every N rows of atoms parallel to the (001) direction are removed to create a $(N\times1)$ missing-row superstructure. This superstructure could be regarded as a set of up-down steps with terraces that are $(N-1)$ atoms wide, separated by a single missing row of atoms. Figure 2 shows the calculated values of ρ_s^{xx} and ρ_s^{yy} for

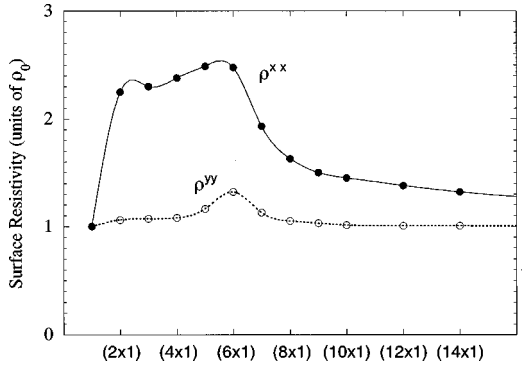

FIG. 2. The calculated surface-induced resistivity for a series of Al(100) $N\times1$ missing-row superstructures. The surface resistivity of the missing-row surface is expressed in units of the surface resistivity of the (flat) Al(100) surface, ρ_0. Solid circles: the *xx* component of the surface resistivity tensor corresponding to the resistivity of the surface when the current flow and applied field are perpendicular to the step edges. Open circles: the *yy* component of the surface resistivity tensor corresponding to the resistivity of the surface when the current flow and applied field are parallel to the step edges. The lines are guides to the eye only.

these missing row surfaces, plotted as a function of N. In Fig. 3 the surface resistivity is normalized to the surface resistivity of the unstepped (100) surface, ρ_0.

In Fig. 2 we observe several trends. First, we note that for $N=1$, and in the limit $N\rightarrow\infty$, there are no missing rows present on the surface and we would expect that $\rho_s^{xx} = \rho_s^{yy} = \rho_0$. This trend is clearly reproduced in the calculation. Second, surfaces with a relatively high density of missing rows [i.e., $(2\times1)-(6\times1)$] show a substantial increase in ρ^{xx} compared to the Al(100). ρ^{xx} corresponds to the case where rows of atoms are removed perpendicular to the direction of current flow. Clearly, this increase is a result of the additional diffuse scattering of carriers at the (100) surface, generated by the missing row line defects. We observe that, for $N=2-6$, ρ^{xx} is relatively insensitive to the density of the missing rows at the surface. However, for $N\geqslant6$, ρ^{xx} drops as

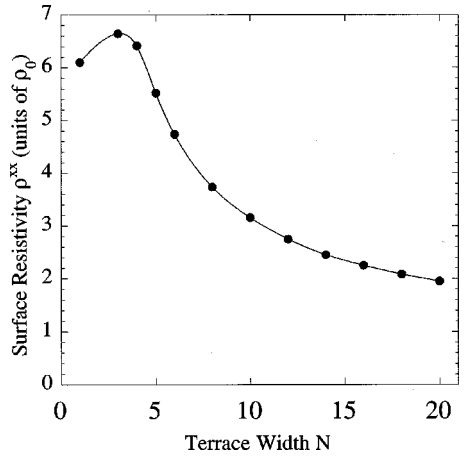

FIG. 3. The calculated *xx* component of the surface-induced resistivity tensor for surfaces vicinal to the Al(100) surface plotted as a function of the terrace width N and normalized to the surface resistivity of the (flat) Al(100) surface, ρ_0. The solid line is a guide to the eye only.

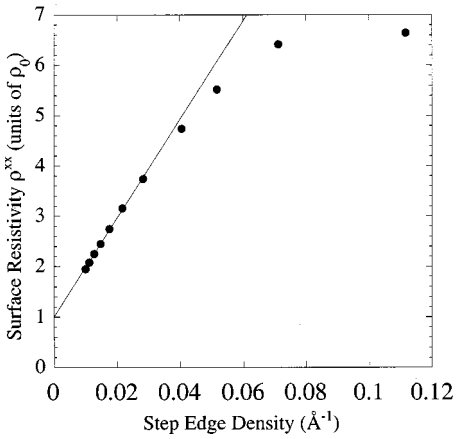

FIG. 4. The calculated *xx* component of surface-induced resistivity tensor for surfaces vicinal to the Al(100) surface plotted as a function of the one-dimensional step-edge density and normalized to the surface resistivity of the (flat) Al(100) surface, ρ_0. The solid line is a linear fit to the low step-density results with slope 98 Å.

the density of missing rows decreases. This latter behavior would be expected in the regime where the missing rows are sufficiently far apart for the diffuse scattering from each line defect to be considered independent of the other missing rows.

From Fig. 2 we observe that, compared to ρ^{xx}, ρ^{yy} is only weakly changed by the presence of the missing row. This reflects the relative ineffectiveness of steps in scattering carriers which impinge parallel to the step edges, an effect also observed in Ishida's calculation for the (4×1) superstructure. For comparison we note that Ishida's pseudopotential calculation[10] for the (4×1) superstructure yielded $\rho_s^{xx}/\rho_0 \sim 2-3.3$. (This range of values arises because in Ishida's calculation ρ_0 and ρ_s^{xx} were computed for two different model surfaces; one-layer and two-layer slabs on jellium, respectively.) Clearly, the substantial increase in the ρ^{xx} observed in the pseudopotential calculation is reproduced by the results shown in Fig. 2.

Next we considered a more realistic set of stepped surfaces; the surfaces vicinal to Al(100) described at the beginning of this section. Figure 3 shows the calculated values of ρ^{xx} for these surfaces plotted as a function of the terrace width, N, and is normalized to the surface resistivity of Al(100). For terrace widths of $N\sim5$ we see that ρ^{xx} is increased by approximately a factor of 6 over its value for Al(100). Again, this increase is a reflection of the additional diffuse scattering of carriers by the step edges. We note that the case of $N=1$ corresponds to the Al(111) surface. As was noted earlier, a first-principles calculation of the surface resistivity of Al(111) and Al(100) by Ishida[12] determined that ρ^{xx} for Al(111) was a factor of 6 larger than for Al(100). That result is clearly consistent with the results shown in Fig. 3.

As the terrace width increases we observe a drop in the surface-induced resistivity towards its value for the unstepped Al(100) surface. This decrease simply reflects the reduction of the spatial density of step edges on the surface as a function of the terrace width. This is more apparent in Fig. 4 where ρ^{xx} is replotted as a function of the one-dimensional step-edge density of the surface η_s (i.e., the number of step edges per unit Å). From Fig. 4 it is apparent that as $\eta_s\rightarrow0$ the surface resistivity becomes a linear function of the step density,

$$\lim_{\eta_s\rightarrow}\frac{\rho_s^{xx}}{\rho_0}=1+\frac{1}{\rho_0}\frac{\delta\rho_{\text{step}}}{\delta\eta_s}\eta_s, \tag{7}$$

where $(1/\rho_0)(\delta\rho_{\text{step}}/\delta\eta_s)$ isolates the contribution to the surface resistivity from the step edges. In this low step-density regime, where the step edges are far apart, it is clear that each step edge makes an independent contribution to the surface resistivity of the stepped surface. This is consistent with a model in which the multiple scattering of carriers between step edges is short range and becomes negligible at sufficiently low step densities. From Fig. 4 we see that this linear dependence is established when the step edges are further than approximately 25 Å apart.

Figure 4 indicates that there is a strong deviation from linearity for higher step-edge densities where the calculated surface resistivity is lower than predicted by a linear extrapolation of the low step-density resistivity. This suggests that the scattering interaction between step edges reduces the net amount of diffuse scattering from the surface so that the surface resistivity is smaller than would be expected from simply superposing the effect of each step edge. This is a manifestation of multiple scattering of the carriers between adjacent step edges; each step edge lies in the ''shadow'' of the upstream step edge(s). Similar behavior has been seen in calculations of the wind force of pairs of adatoms, and adatoms and atom rows.[19] For disordered overlayers of adatoms on metallic substrates this multiple-scattering interaction gives rise to the so-called Nordheim effect in surface resistivity; the parabolic dependence of the ρ_s which rises and then falls as the adatom coverage is varied between $\theta=0$ and 1.[2] Figure 4 shows that there also exists similar behavior in the surface resistivity of stepped surfaces. However, there is a fundamental difference between the step and adatom case. For stepped surfaces, the zero $(N=\infty)$ and unit $(N=1)$ coverage limits correspond to two different low Miller index surfaces, Al(100) and Al(111), respectively. Therefore, unlike the adatom case (where $\theta=0$ and 1 correspond to the same surface), the surface resistivity of a stepped surface at zero and unit step-edge coverage will not, in general, be the same.

In the low step-density regime, we deduce from the linear fit shown in Fig. 4 that $(1/\rho_0)(\delta\rho_{\text{step}}/\delta\eta_s)\sim98$ Å. This quantity is a measure of the contribution of a single Al(100) step to the surface resistivity of a stepped Al(100) surface. It has a simple physical interpretation in the low step-density regime. When compared to the unstepped Al(100) surface, it is the average distance between step edges that doubles the surface resistivity.

Given this interpretation of the variation of ρ_s with the step-edge density, we now return to the missing-row results presented earlier (Fig. 2) and in Fig. 5 we replot ρ^{xx} as a function of the one-dimensional missing-row density. Comparing Fig. 5 (missing rows) to Fig. 4 (step edges) we observe that, when the missing-row density is low, the surface-induced resistivity depends linearly upon the density of missing rows. Then, each missing row makes an independent contribution to ρ_s. As in the step case (Fig. 4), a deviation

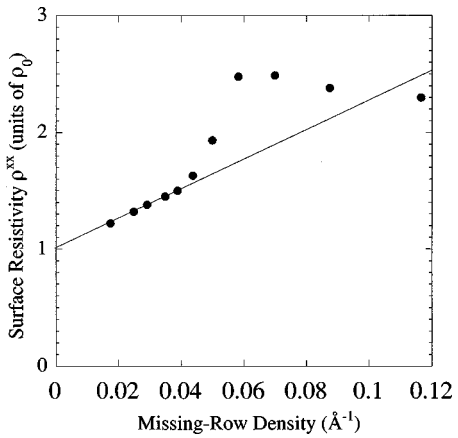

FIG. 5. The calculated *xx* component of the surface-induced resistivity tensor for a series of Al(100) $N\times 1$ missing-row superstructures, plotted as a function of the missing-row density. The solid line is a linear fit to the low density results with slope 13 Å.

from linearity occurs for higher missing-row densities. However, in contrast to the stepped surface, in this case ρ_s rises above the value predicted by a linear dependence. This difference is a consequence of the scattering interaction between rows of vacancies, rather than the rows of atoms which constitute the step edges, which tends to increase the diffuse scattering from the surface. We deduce from the linear fit shown in Fig. 5 that for an isolated missing row $(1/\rho_0)(\delta\rho_{mr}/\delta\eta_s)\sim 13$ Å. This value is significantly smaller than that obtained for a single step edge, 98 Å.

It is informative to compare the contribution to ρ_s from an isolated step edge or missing row to that from an isolated Al adatom on Al(100), $l_f\rho_a$, where l_f is the film thickness. In the limit of low adatom coverage

$$[l_f\rho_a]=\frac{n_a Z_w}{n_e}, \tag{8}$$

where n_a is the two-dimensional adatom density at the surface, n_e is the carrier density and Z_w is the adatom wind valence. This relation is strictly valid only for jellium where all the momentum transfer occurs between the adatom and the carriers. Nevertheless, we may use Eq. (8) to estimate the contribution to the surface resistivity of a single row of adatoms, with the same interatomic spacing as the rows of atoms parallel to the step edges or missing rows, on Al(100), $a_0=2.86$ Å. Assuming that there is no scattering of carriers between atoms in the row, using the calculated wind valence of an isolated Al adatom (monomer) on semi-infinite jellium,[20] $Z_w=-30e$, we obtain $\rho_{\rm row}/\rho_0\sim 64$ Å. Therefore, the contribution to the surface resistivity from an isolated step on Al(100) is approximately a factor of 1.5 greater than for a single atom row. This suggests that the diffuse scattering of carriers produced by a step is generated within the first one or two rows of atoms at the leading edge of the step. By contrast, the contribution to the surface resistivity from an isolated missing row on Al(100) is approximately a factor of 5 smaller than for a single row of adatoms.

IV. CONCLUSIONS

We have used a multiple-scattering model to compute the surface resistivity of steps vicinal to Al(100). We find that the surface resistivity is a function of the step density, η_s, and becomes a linear function of η_s for low step-edge densities. In this regime the contribution of a step to the surface resistivity can be described by an effective length $\delta\rho_{\rm step}/\delta\eta_s$ which is the average terrace width of a stepped surface that doubles the surface resistivity. For noninteracting steps on Al(100) $(1/\rho_0)(\delta\rho_{\rm step}/\delta\eta_s)\sim 98$ Å. This value is a factor of approximately 1.5 larger than for a single row of Al adatoms aligned parallel to the step edge suggesting that the diffuse scattering of carriers produced by a step occurs within the first one or two rows of atoms at the leading edge of the step.

ACKNOWLEDGMENT

This work has been supported by the NSF-MRSEC Grant No. DMR-96-32521.

*Also at: Department of Physics, University of Maryland Baltimore County, Baltimore, MD 21250.

[1] J. W. Geus, in *Chemisorption and Reactions On Metallic Films*, edited by J. Anderson (Academic, New York, 1971), p. 391.
[2] D. Schumacher, *Surface Scattering Experiments with Conduction Electrons*, Springer Tracts in Modern Physics, Vol. 128 (Springer-Verlag, Berlin, 1993).
[3] D. Lessie and E. Crosson, J. Appl. Phys. **59**, 504 (1986).
[4] B. Persson, Phys. Rev. B **44**, 3277 (1991).
[5] B. Persson, *Sliding Friction* (Springer, New York, 1999).
[6] H. Ishida, Surf. Sci. **363**, 354 (1996).
[7] P. S. Ho and T. Kwok, Rep. Prog. Phys. **52**, 301 (1989).
[8] R. Hummel and H. Huntington, *Electro- and Thermo-transport in Metals and Alloys* (American Institute of Mining, Metallurgical and Petroleum Engineers, Pittsburgh, 1977).
[9] A. Kaser and E. Gerlach, Z. Phys. B: Condens. Matter **97**, 139 (1995).
[10] H. Ishida, Phys. Rev. B **52**, 10 819 (1995).
[11] P. J. Rous, Phys. Rev. B **59**, 7719 (1999).
[12] H. Ishida, Phys. Rev. B **57**, 4140 (1998).
[13] D. Bly and P. J. Rous, Phys. Rev. B **53**, 13 909 (1996).
[14] N. Cabrera, V. Celli, F. Goodman, and R. Manson, Surf. Sci. **19**, 67 (1970).
[15] N. Garcia and N. Cabrera, Phys. Rev. B **18**, 576 (1978).
[16] N. Garcia, J. Chem. Phys. **67**, 897 (1977).
[17] T. Engel and K. Rieder, *Structural Studies of Surfaces with Atomic and Molecular Beam Diffraction*, Springer Tracts In Modern Physics, Vol. 91 (Springer, Berlin, Heidelberg, New York, 1981).
[18] M. A. Van Hove and C. M. Chan, *Low-Energy Electron Diffraction* (Springer-Verlag, Berlin, 1986).
[19] D. Bly, Ph.D. thesis, University of Maryland, Baltimore County, 1996.
[20] H. Ishida, Phys. Rev. B **49**, 14 610 (1994).